Physicochem. Probl. Miner. Process., 60(4), 2024, 190698

http://www.journalssystem.com/ppmp

Physicochemical Problems of Mineral Processing

ISSN 1643-1049

The inhibition mechanism of esterified starch on flotation separation of fluorite and calcite

Bangqi Wei [1], Jie Li [2], Zhao Cao [1], Saisai Ma [1], Yuhan Zhang [3]

[1] School of Mining and Coal, Inner Mongolia University of Science and Technology, Baotou, China

[2] School of Rare Earth Industry, Inner Mongolia University of Science and Technology, Baotou, China

[3] School of Energy Science and Environment, Inner Mongolia University of Science and Technology, Baotou, China

Corresponding author: yjslijie@sohu.com (Jie Li)

Abstract: Herein, the flotation behavior of fluorite and calcite was examined before and after starch esterification through mineral flotation experiments. Moreover, the adsorption action mechanisms on minerals before and after starch esterification were investigated using methods such as solution surface tension measurement, infrared spectroscopy, and extended Derjaguin–Landau–Verwey–Overbeek theory. The results showed that after starch esterification (esterified starch), there was a greater difference in the mineral recovery rate compared to before starch esterification (ordinary starch), with a better inhibition effect on calcite. The interaction between mineral surfaces and ordinary starch was weaker than the interaction between minerals and esterified starch. In particular, after starch esterification, the surface tension increased, two minerals contact angle decreased, the surface potential became more negative, and the difference in the mineral recovery rate was greater than before starch esterification. After the interaction between minerals and esterified starch, calcite particles displayed good dispersibility, while the cohesion between calcite particles and sodium oleate particles decreased; notably, the effect on fluorite was opposite. Calcite and esterified starch exhibited chemical adsorption, impeding the adsorption of sodium oleate onto calcite and resulting in calcite inhibition. The interaction between fluorite surface and esterified starch involved electrostatic adsorption, with sodium oleate chemically adsorbed onto the fluorite surface. Chemical adsorption proved stronger than electrostatic adsorption, enabling sodium oleate to capture fluorite.

***Keywords*:** mineral flotation, esterified starch, surface tension, EDLVO theory

1. Introduction

Fluorite, a mineral abundant in fluorine, finds extensive applications in industries such as metallurgy and pharmaceuticals (Corpas et al.,2020). As the global economy continues to evolve and resource exploration deepens, the demand for fluorite is also steadily increasing, emphasizing the importance of its rational exploitation and utilization (Gao et al., 2021; Shang et al., 2020). Typically, most fluorite resources are found in association with gangue minerals, featuring varying mineral concentrations ranging from abundant to scarce (Zhao et al., 2020). The majority of associated fluorite deposits are calcite-type fluorite ore (Wang et al., 2018). Calcite shares similar surface properties with fluorite, posing a persistent challenge in its flotation separation within the mineral processing industry (Sun et al., 2021). Common inhibitors for calcite include sodium silicate, sodium hexametaphosphate, tannic acid, and sodium carboxymethyl cellulose (Lu et al., 2023; Feng et al., 2011). Given the environmental considerations in the mineral processing industry, there is a pressing need for efficient and environmentally friendly calcite inhibitors.

Starch inhibitors, being natural polymer organic compounds, offer advantages such as green environmental protection and cost-effectiveness, and they find widespread application in mineral flotation and other related fields (Wang et al., 2023; Zhang et al., 2023; Dong et al., 2010). Wang (Wang, 2023) utilized oxidized starch as an inhibitor and sodium oleate as a collector for the flotation separation of calcite-type fluorite ore. Research indicates that the addition of oxidized starch substantially decreases the electrokinetic potential of calcite, while having minimal impact on the electrokinetic

DOI: 10.37190/ppmp/190698

potential of fluorite, thereby facilitating the separation of fluorite and calcite. Wang et al. (Wang et al., 2023) employed Al-starch as a calcite inhibitor for flotation tungsten concentrate. Experimental results demonstrate that Al-starch selectively adsorbs onto the oxygen sites of carbonate anions on the calcite surface via metal groups without interacting with the scheelite surface, consequently modifying the surface charge and characteristic atoms of calcite, thereby exerting inhibitory effects.

Esterified starch falls under the category of starch inhibitors, yet there is limited literature on its application in the flotation separation of fluorite and calcite minerals. Therefore, this study integrates mineral experiments with theoretical analysis to investigate the effects of starch esterification on the flotation separation of fluorite and calcite in the presence of sodium oleate as a collector. The present work delves into the effect of citric acid esterified starch on the flotation separation of fluorite and calcite, marking the first exploration of its kind. It is of great significance of esterified starch for the flotation separation of fluorite and calcite to elucidate the inhibition mechanism.

2. Materials and methods

2.1. Materials

The fluorite and calcite samples utilized in the experiment were all sourced from Hunan Shizhuyuan Nonferrous Metals Co., Ltd., China, with a purity of > 95%. Hand-selected pure ore blocks of fluorite and calcite were used, which were crushed by hammering, picked up with tweezers to remove impurities, and then repeatedly rinsed with deionized water. Subsequently, they were dried in an electric blast constant-temperature drying oven (101-2A) at a low temperature. Then, the samples were ground using a three-head grinder and sieved to obtain particles with a size range of 38–74 μm. Following another round of low-temperature drying, they were stored in a grinding bottle for future use. Table 1 lists the chemical composition details.

Table 1. Analysis results of the main chemical components of fluorite and calcite single minerals

mineral	Content of each major component（%）				
	CaF_2	CaO	MgO	SiO_2	Al_2O_3
fluorite	99.68	-	0.028	0.113	0.025
calcite	-	54.26	0.384	0.215	0.032

According to the X-ray diffraction (XRD) spectrum analysis, it was observed that the diffraction peaks of the two mineral samples coincided with their standard diffraction peaks without obvious impurity peaks. This indicates that the purity of fluorite and calcite minerals was high, which could be considered pure minerals and met the requirements of mineral flotation tests. As the mineral crystal planes possess anisotropy, the experimental minerals were analyzed by XRD patterns, and the fluorite (111) crystal planes and calcite (104) crystal planes were the exposed surfaces with the lowest energy for mineral fragmentation (Gao et al., 2016). The XRD spectrum of the sample is shown in Fig. 1.

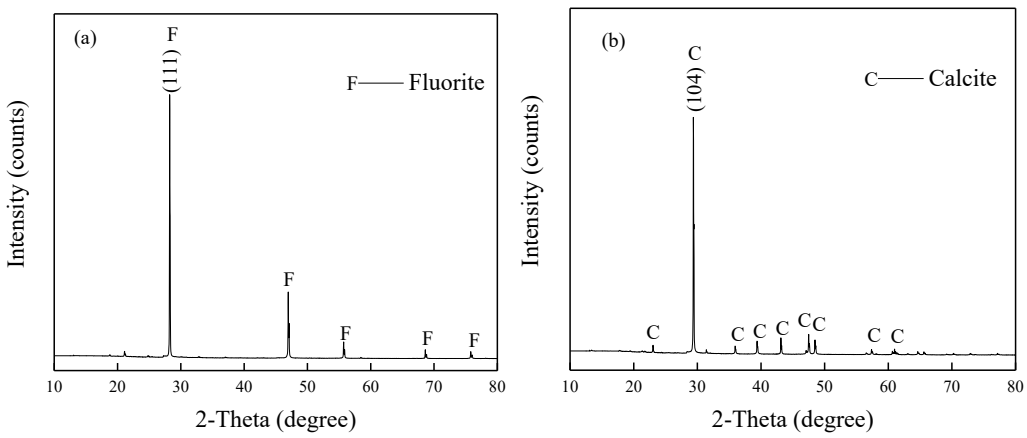

Fig. 1. X-ray diffraction patterns of fluorite and calcite

The chemicals used in the experiments were all of analytical grade purity. Esterified starch was synthesized by the dry method (Ning et al., 2021; Yu, 2008). Citric acid measuring 0.6 g was accurately weighed and heated with a minimal amount of deionized water to aid in dissolution. Subsequently, the pH value was adjusted to approximately 3 using 10mol/L sodium hydroxide. A total of 2 g of corn starch (Hefei Jinu Biotechnology Co., Ltd., China) was weighed and thoroughly mixed with 3 mL of ethanol and the prepared citric acid solution. The mixture was then allowed to stand at room temperature for 30 min. Then, the starch mixture was placed in a drying oven and dried at 90°C for 6 h. After removal, it was crushed, washed with deionized water to eliminate unreacted citric acid, and filtered. It was then air-dried at room temperature, crushed again, and packaged.

2.2. Flotation experiment

The flotation test was conducted using the inflatable hanging trough flotation machine (XFC-type), employing a 30mL flotation cell with an adjusted speed of 1992 r/min. For single mineral flotation or artificial mixed mineral samples (1g fluorite + 1g calcite), 2.00 g of the ore sample (38–74 μm) was weighed each time and transferred to a 30mL flotation cell; deionized water was added, and the mixture stirred for 2 min. Starch was added, followed by pH value adjustment using a pH regulator and stirred for 3 min. Sodium oleate was added, stirred for 3 min, followed by manual scraping for 3 min. The flotation concentrate and tailings were filtered, dried, weighed, calculated, and then stored in bags for backup.

2.3. Surface tension and contact angle testing

Surface tension was measured using the ring method (Wang et al., 2021; Chen et al., 2011), employing the KRÜSS K100 surface tension and contact angle measuring instrument. The H&J correction method was used, with a sampling interval of the position step set at 0.05 mm. The contact angle measurement was performed based on the capillary constant of n-hexane, with a section of data from a straight rise selected for automatic fitting calculation in the final results.

2.4. Zeta potential test

The Zeta potential of the mineral surface was measured using the Bruker Brookhaven Zeta Plus analyzer. The mineral sample was ground to a fine −5μm size. Two hundred milligrams of the sample was accurately weighed and placed in a beaker. Deionized water and reagents were added to replicate the conditions of the flotation test. The mixture was stirred with a magnetic stirrer for 5 min, allowed to settle, and the supernatant was then extracted for analysis. Each sample underwent three automatic measurements and the average value was recorded.

2.5. Fourier-transform infrared spectroscopy analysis

Fourier-transform infrared (FTIR, Bruker VETEX 70) spectroscopy was used for detection. First, the infrared spectrum of the reagent was measured, and the mineral sample that interacted with reagent was then ground to −10 μm. This prepared sample was mixed with spectrally pure potassium bromide at a 1:150 ratio, followed by compression testing.

2.6. Extended Derjaguin–Landau–Verwey–Overbeek (EDLVO) theory

The classic Derjaguin–Landau–Verwey–Overbeek (DLVO) theory fails to adequately elucidate the agglomeration behavior of particles in the presence of flotation agents. Numerous studies have demonstrated that particle interactions in sol dispersion systems also include interfacial polar interaction energy. Consequently, EDLVO theory is required to explain the aggregation behavior of particles in sol systems. The total energy of particle interactions is expressed by the following equation (Wang et al., 2016; Ren, 2012; Vilinska and Rao, 2011; Hu et al., 1994; Hu et al., 1993). According to the literature records (Wang et al., 2016; Hu et al., 1994), the Hamaker constant A_{11} of fluorite is 7.2×10^{-20} J; the Hamaker constant A_{22} of calcite is 12.4×10^{-20} J. The mineral particle size is determined to be 50 μm, and the sodium oleate particle size is 7.5 μm.

$$V_T^{ED} = V_E + V_W + V_{HA} \quad (1)$$

$$V_W = -\frac{A}{6H} \cdot \frac{R_1 R_2}{R_1 + R_2} \tag{2}$$

Homogeneous particles:

$$V_E = 2\pi\varepsilon_a R\varphi_0^2 \ln[1 + exp(-kH)] \tag{3}$$

Heterologous particles:

$$V_E = \frac{\pi\varepsilon_a R_1 R_2}{R_{1+}R_2}\left(\varphi_1^2 + \varphi_2^2\right)\left(\frac{2\varphi_1\varphi_2}{\varphi_1^2 + \varphi_2^2}p + q\right) \tag{4}$$

$$V_{HA} = 2\pi\frac{R_1 R_2}{R_1 + R_2}h_0 V_{HA}^0 exp\left(-\frac{H}{h_0}\right) \tag{5}$$

In the formula, V_T^{ED} represents the total EDLVO potential energy of the interaction between particles, J; V_E denotes the electrostatic interaction energy of the double layer, J; V_W represents the van der waals interaction energy, J; V_{HA} is the interfacial polar interaction energy, J; R_1 and R_2 are the radii of different particles, nm; H indicates the spacing between particles, nm; A is the effective Hamaker constant between particles in the medium, J; φ is the surface potential of the particle (represented by Zeta potential here, as depicted in Table 2); k is the Debye length, 0.023 nm; ε_a is the absolute dielectric constant of the dispersed medium, 6.95×10^{-10} C^2/J m; h_0 is the attenuation length, 1 nm; V_{HA}^0 represents the interaction energy constant, mJ/m^2.

Table 2. Zeta potential of particles

Type	Zeta potential (mV)	Type	Zeta potential (mV)
fluorite	10.14	calcite	4.48
fluorite+ ordinary starch	7.38	calcite+ ordinary starch	-14.46
fluorite+ esterified starch	3.95	calcite+ esterified starch	-16.59
sodium oleate	-17.54	sodium oleate+ ordinary starch	-20.30
-	-	sodium oleate+ esterified starch	-23.73

3. Results and discussions

3.1. Mineral flotation test

3.1.1. Effect of sodium oleate on the floatability of single minerals

Fig. 2 illustrates the investigation of the effect of sodium oleate dosage on the collection ability of fluorite and calcite at a pH value of 7. The figure shows that at a pH value of 7, the flotation recovery rate of minerals increased as the sodium oleate dosage increased. Due to the Ca^{2+} particle density on the exposed surface of fluorite (111) being 12.9 μmol/m^2 and calcite (104) being 8.24 μmol/m^2, the adsorption site density on the surface of fluorite was higher than that of calcite (Gao et al., 2016), resulting in a higher recovery rate of fluorite. When the sodium oleate dosage was 15 mg/L, both fluorite and calcite achieved high recovery rates and began to stabilize. Therefore, the sodium oleate dosage for subsequent experiments was determined to be 15 mg/L.

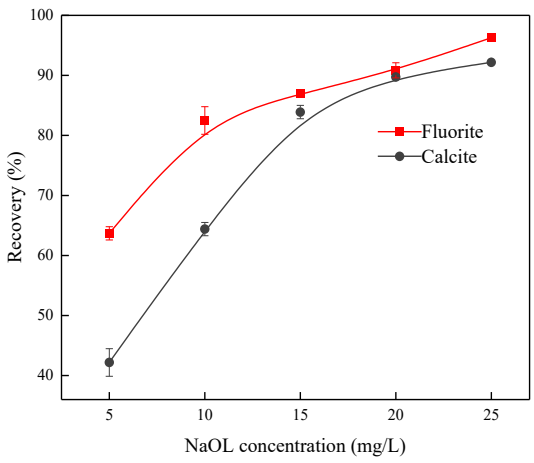

Fig. 2. Effect of sodium oleate on flotation recovery of fluorite and calcite

3.1.2. Effect of starch on the flotation performance of single minerals

In a flotation system with 15mg/L sodium oleate, a neutral environment with a pH value of 7 was chosen to examine the inhibitory effect of the dosage of inhibitors on two calcium-containing minerals, fluorite and calcite. Figs. 3 (a) and (b) show that in a neutral environment with pH 7, the flotation recovery rate of fluorite slightly decreased with the increase with both types of starch dosage, the magnitude was not significant. The recovery rate of calcite sharply decreased and eventually tended to flatten out. From the comparison between Figs. 3 (a) and (b), it can be observed that when the starch amount reached 40 mg/L, esterified starch resulted in a recovery rate of 23.62% for calcite, and ordinary starch resulted in a recovery rate of 39.18% for calcite. Notably, esterified starch had a better inhibitory effect on calcite flotation.

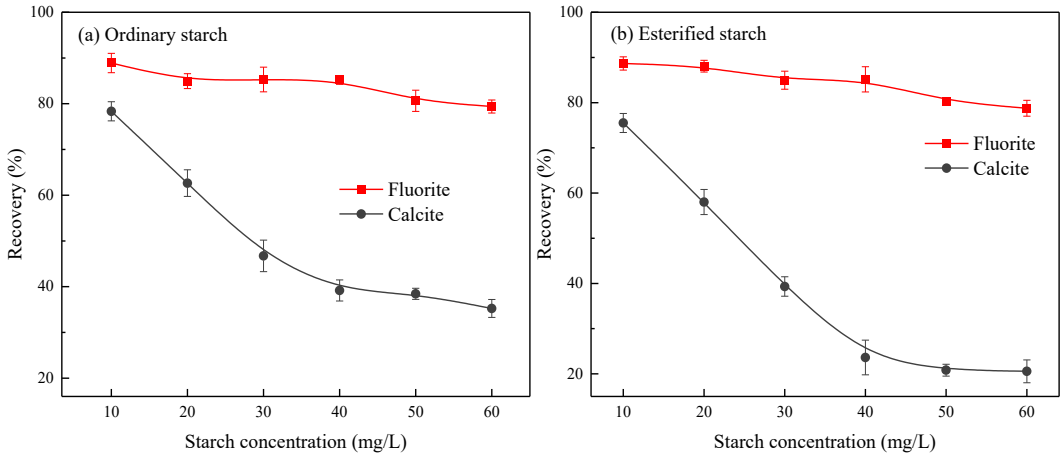

Fig. 3. Effect of the dosage starch on the flotation recovery rate of fluorite and calcite

3.1.3. The effect of pulp on single mineral flotation performance in different pH environments

A fixed sodium oleate dosage of 15 mg/L and a starch dosage of 40 mg/L were used to investigate the effect of pulp pH value on the flotation performance of single minerals. The results are shown in Fig. 4. Due to the calcite dissolution in acidic media, experiments were only conducted in environments with a pH value of ≥7. Figs. 4 (a) and (b) show that under acidic or alkaline conditions, the recovery rate of fluorite decreased, which was not conducive to the flotation recovery of fluorite. Under alkaline conditions, the recovery rate of calcite did not change much and remained relatively low. Comparing Figs. 4 (a) and (b), when pH is 7, the difference in recovery rates between fluorite and calcite is the greatest, with fluorite at 85.16% and calcite at 23.62%. Hence, in the single mineral flotation test, the recovery rate of fluorite was most affected by the pH value of the slurry. In a neutral slurry environment, starch esterification facilitated a more effective separation of fluorite and calcite.

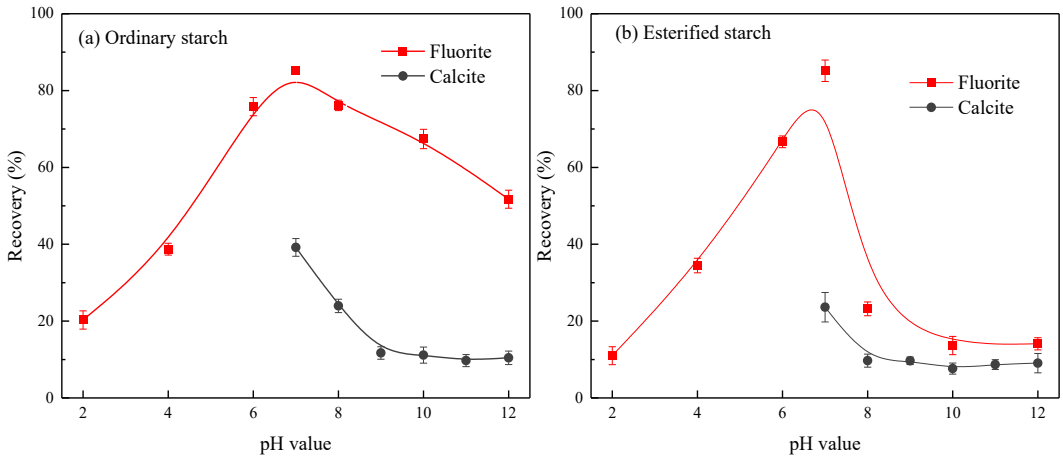

Fig. 4. Effect of different pH values of pulp on the recovery of calcite and fluorite

3.1.4. Artificially mixed ore experiment

When the pH value of the slurry was 7, the sodium oleate dosage was 15 mg/L, and the starch dosage was 40 mg/L. The separation effect of artificially mixed ore was compared, and the results are shown in Table 3.

The flotation effect of artificially mixed ore showed that the fluorite grade was 68.54%, when ordinary starch was used as an inhibitor. The recovery rate of fluorite was 44.16%, which was a low result. The low recovery rate of fluorite can cause resource waste. Nevertheless, when esterified starch was used as an inhibitor, the fluorite grade increased to 80.90%, marking a notable increase of 12.36%, and the recovery rate was also enhanced. This suggests that starch esterification had a good separation effect on fluorite and calcite.

Table 3. Flotation effect of artificially mixed ore before and after starch esterification / (%)

Product (concentrator)	Total recovery rate	Fluorite grade	Fluorite recovery
Ordinary starch	32.22	68.54	44.16
Esterified starch	49.35	80.90	79.85

3.2. Mechanism analysis

3.2.1. Contact angle test

In Fig. 5 (a), it can be observed that in the absence of depressants, an increase in the amount of sodium oleate led to an increase in the contact angle of fluorite and calcite. This suggests that both minerals exhibited good floatability in sodium oleate solution. Moreover, the contact angle of fluorite was greater than that of calcite. In Fig. 5 (b), it is evident that at a sodium oleate concentration of 15 mg/L, the contact angle of the mineral surface decreased after the addition of starch compared to its state before the starch addition. After the interaction between starch and mineral surfaces resulted in a small change in the contact angle of fluorite while a large change in the contact angle of calcite. The effect of esterified starch on mineral contact angle was greater than that of ordinary starch on mineral contact angle.

At an esterified starch concentration of 40 mg/L, the contact angle of calcite measured 58.56°. In comparison to the contact angle of minerals at a sodium oleate concentration of 15 mg/L (as shown in (a)), it is evident that esterified starch reduced the contact angle of calcite by 12.05°. The reduction in the contact angle of calcite enhances its hydrophilicity, thereby resulting in a lower recovery rate. The contact angle of the fluorite also decreased, but the decrease was not significant, manifested by a slight change in the recovery rate. These findings align with the results of mineral flotation experiments.

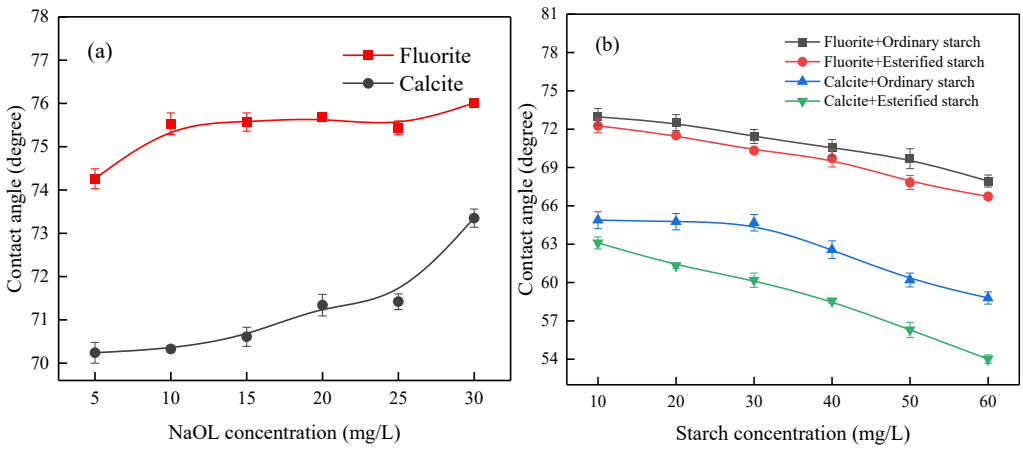

Fig. 5. Contact angle between fluorite and calcite under different conditions

3.2.2. Surface tension test

The surface tension of the solution is a crucial control parameter in flotation, which directly affects the flotation recovery rate of minerals. The surface tension of the collector solution and the mixed flotation

solution reagent solution at a concentration of 15 mg/L of sodium oleate were tested. As shown in Fig. 6 (a), with the increase of sodium oleate concentration, the surface tension of the solution decreased. At a sodium oleate concentration of 15 mg/L, the surface tension measured 39.11 mN/m. As shown in Fig. 6 (b), after adding starch, the surface tension of the original 15mg/L sodium oleate solution increased. With rising starch concentration, the surface tension of the solution initially decreased and then it tended to flatten out. Adding starch resulted in a critical micelle concentration of 40 mg/L for the mixed solution, with the surface tension of the esterified starch mixed solution being higher than that of ordinary starch solution. The introduction of –COOH in esterified starch increased the solution's polarity, intermolecular attraction, and surface tension compared to the ordinary starch solution increased (Timothy et al., 2008). The greater the surface tension, the more unstable the bubbles become (Hadler and Cilliers, 2019), thus reducing bubble stability and mineral adsorption on the surface of the bubbles, which decreases the recovery rates of fluorite and calcite.

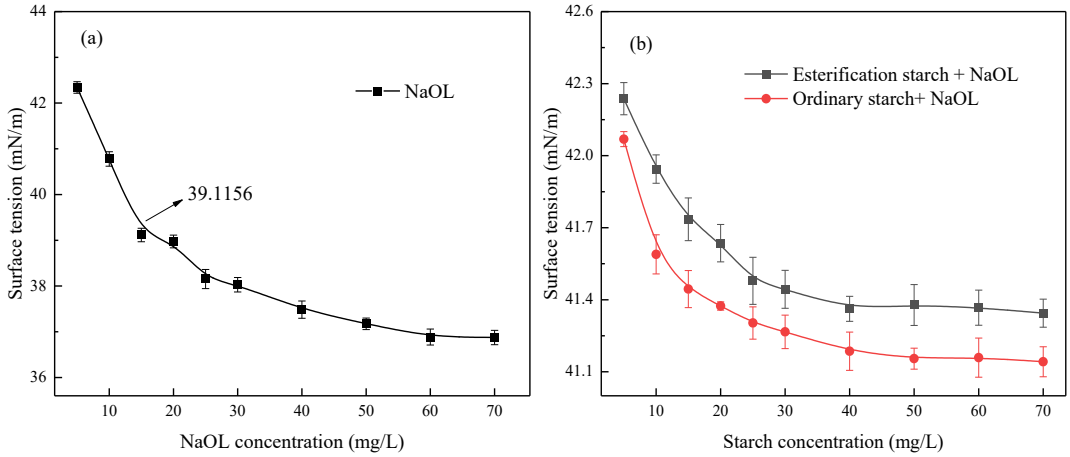

Fig. 6. Surface tension of solutions at different concentrations

3.2.3. Zeta potential test

Zeta potential tests were conducted on minerals in a slurry at various pH values with a starch concentration of 40 mg/L to further elucidate the effect of starch on the surface properties of fluorite and calcite. As shown in Fig. 7, the zero potential of fluorite and calcite was around 7.4 and 7.3, respectively. Due to the large negative value of the hydration-free energy of anions on the mineral surface, anions on the mineral surface were preferentially transferred to the aqueous solution, and the mineral surface was positively charged (Shen, 2017). Ordinary starch was adsorbed on the surface of minerals, causing a decrease in fluorite and calcite mineral surface potential. Introducing –COOH to the starch structure resulted in stronger polarity and electronegativity of esterified starch (Janine et al., 2020; Chen, 2019; Zhong et al., 2017), leading to a further decrease in the surface potential of the mineral. After the interaction between esterified starch and fluorite, the Zeta potential on the mineral surface decreased in a small range. In an environment with a pH value of 7, the potential value remained positive, allowing it to combine with anionic collectors. The potential showed a negative value after the interaction between esterified starch and calcite. In esterified starch, the potential value decreased even further, causing calcite particles to repel each other due to their negative charge, which is less favorable for binding with anionic collectors.

3.2.4. FT-IR analysis

The changes in functional groups before and after starch esterification can be analyzed by infrared spectroscopy (Fig. 8). The surface interaction mode between starch and minerals can be explored by analyzing the changes in the infrared absorption peaks before and after the interaction between starch and minerals. The test results are shown in Fig. 9 and Fig.10.

As shown in Fig. 8, characteristic peaks of sugars appeared at 2931.78, 1649.12, and 989.47 cm^{-1} before and after starch esterification (Xie et al., 2001). Comparing the curves a1 and b1, the esterified starch exhibited a sharp ester bond (C=O) stretching symmetric absorption peak at 1735.92 cm^{-1}. This indicates that the starch molecule was successfully integrated into the ester group. Starch is a macromolecular

inhibitor with a high degree of molecular polymerization. For the convenience of research, glucose units of starch molecules were used for analysis. Before and after starch esterification, owing to the existence of free –OH at the C2, C3, and C6 positions in its molecular structure, the steric hindrance of the –OH group at position C6 was minimal, leading to the occurrence of a substitution reaction first (Ning et al., 2021).

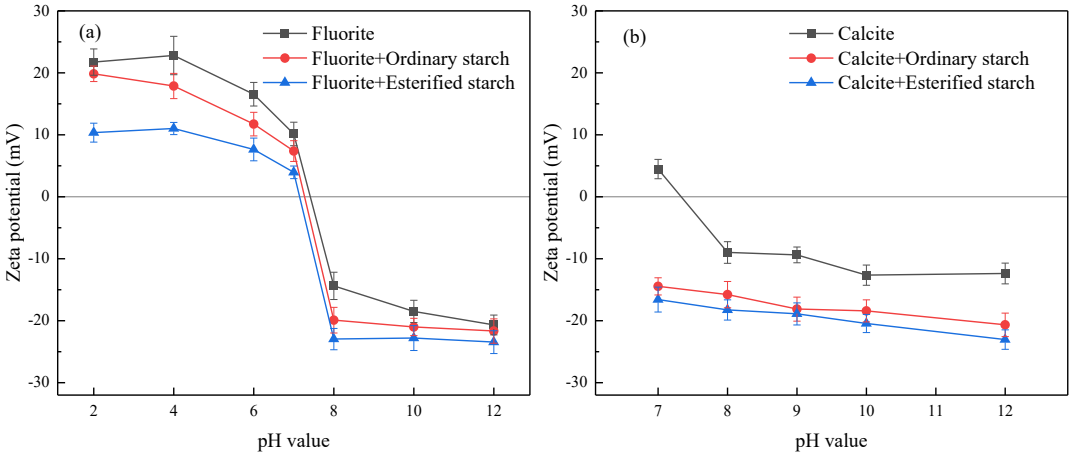

Fig. 7. Effect of different environments on the surface potential of fluorite and calcite

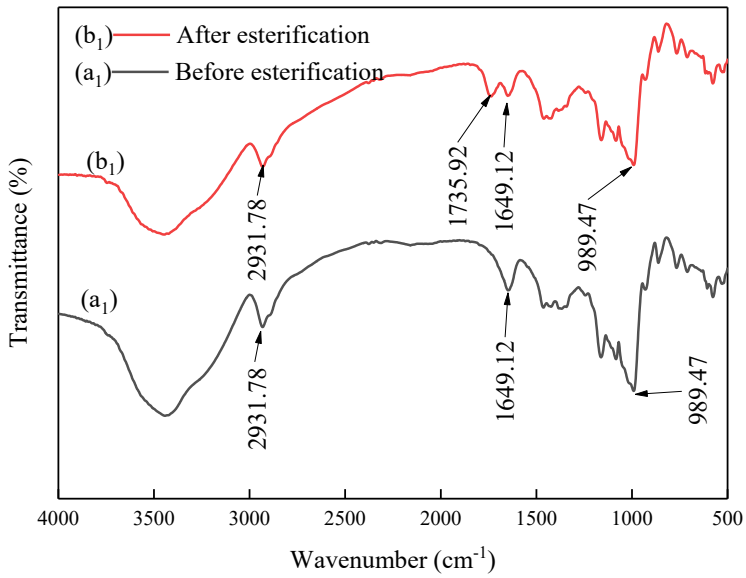

Fig. 8. Infrared spectrum before and after starch esterification

The characteristic absorption peaks of fluorite can be observed at 3442.91, 1625.98, and 1456.24 cm^{-1} in Fig. 9 (Zhu et al., 2021). Following the interaction between ordinary starch and fluorite, a sugar C–O stretching symmetric absorption peak appeared at 1130.26 cm^{-1}, indicating the adsorption of starch on the fluorite surface. When compared to the infrared spectrum of fluorite treated with ordinary starch, the infrared spectrum of fluorite treated with esterified starch also exhibited a sugar C–O stretching symmetric absorption peak at 1130.26 cm^{-1}. This suggests a similar adsorption pattern on the surface of fluorite before and after starch esterification. Compared to the three curves in Fig. 9, there was no obvious redshift or blue shift in the peak position, and the intensity of the new absorption peak was not significant. This suggests that the adsorption on the surface of fluorite both before and after starch esterification was primarily electrostatic (Zhu et al., 2021; Li et al., 1996).

Sodium oleate was chemically adsorbed onto the surface of fluorite (Lu et al., 2023), with the C-H bond on the oleate ion chain being non-polar and resistant to breakage. On the surface of fluorite (111), the F- density was greater than the Ca^{2+} density. Additionally, during adsorption, H^{+} formed strong electrostatic adsorption with F^{-}, enhancing the stability of the adsorption process. Consequently, the stability of sodium oleate adsorption on the surface of fluorite was stronger than that of starch.

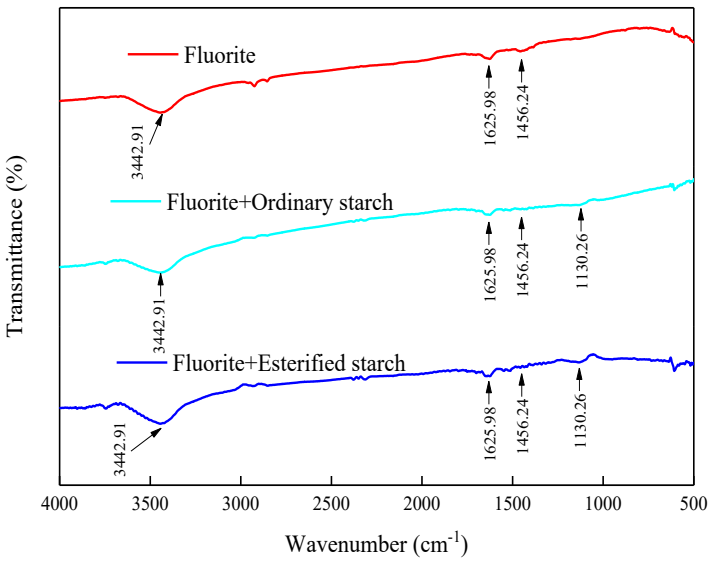

Fig. 9. Infrared spectra before and after the interaction between starch and fluorite

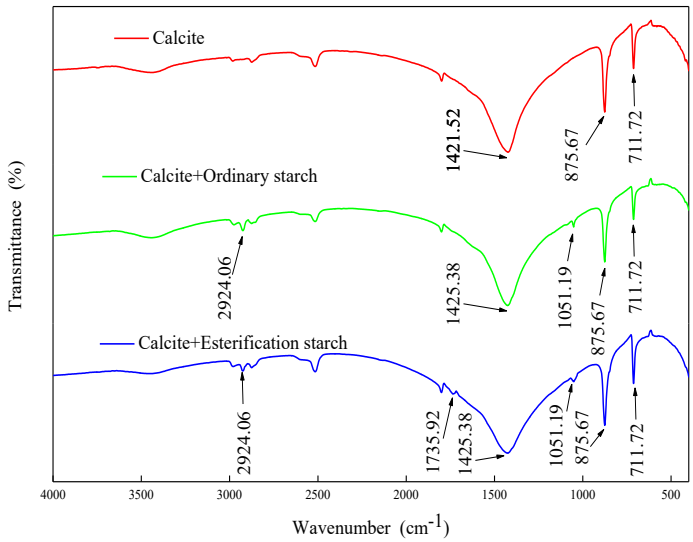

Fig. 10. Infrared spectra before and after the interaction between starch and calcite

The characteristic absorption peaks of calcite can be observed at 711.72, 875.67, and 1421.52 cm^{-1} in Fig. 10 (Xie et al., 2001). Following the interaction between ordinary starch and calcite, multiple sugar C–O stretching symmetric absorption peaks emerged on the calcite surface near 1051.19 cm^{-1}, and the stretching vibration absorption peak of sugar C–H emerged at 2924.06 cm^{-1}. The characteristic absorption peaks of calcite at 1421.52 cm^{-1} on the surface shifted, indicating the chemical adsorption of ordinary starch on the calcite surface (Young and Millr, 2001). The calcite surface treated with esterified starch exhibited a C=O stretching symmetric absorption peak at 1735.92 cm^{-1}. Characteristic peaks of carbohydrate C-O and C-H also appeared near 1051.19 and 2924.06 cm^{-1}. The characteristic absorption peaks at 1421.52 cm^{-1} on the calcite surface showed a redshift, indicating the chemical adsorption of esterified starch on the calcite surface.

The O-H bond on the molecular structure of ordinary starch is prone to electron splitting in the slurry. Consequently, the unipolar group O atom at the C6 position of ordinary starch tends to undergo single-coordinate adsorption on the surface of calcite minerals. The O atom containing the –COOH bipolar group in esterified starch exhibited a tendency for double coordination adsorption on the surface of calcite minerals. The stability of double-coordinated adsorption surpasses that of single-coordinated adsorption (Liu et al., 2021; Mann, 1988). Esterified starch had better adsorption properties than ordinary starch. Therefore, esterified starch and sodium oleate would compete for adsorption on the calcite surface. Esterified starch was primarily chemically adsorbed on the calcite surface, with a

large number of polar groups on the molecular chain. Polar groups relied on hydrogen bonding to interact more strongly with the O atom on the mineral surface in an aqueous solution. Due to its large molecular size and high steric hindrance (Gao et al., 2018; Hu et al., 2012; Leeuw et al.,1998; Lin and Wang, 1994), esterified starch reduced sodium oleate adsorption on its surface, leading to a decreased recovery rate of calcite.

3.2.5. EDLVO theory

EDLVO calculations were performed under neutral conditions according to formula. Fig. 11 (a) demonstrates that in a neutral environment, before starch was added, the total potential energy between fluorite particles at close range was negative, indicating strong mutual attraction. But when the distance between mineral particles was greater than 5.3 nm, the total potential energy became positive, indicating that the repulsion between fluorite particles began to increase. After adding starch, the esterified starch lowered the total potential energy of the system to a level approaching 0, indicating weaker dispersibility. This could result in mineral entrainment flotation during experiments.

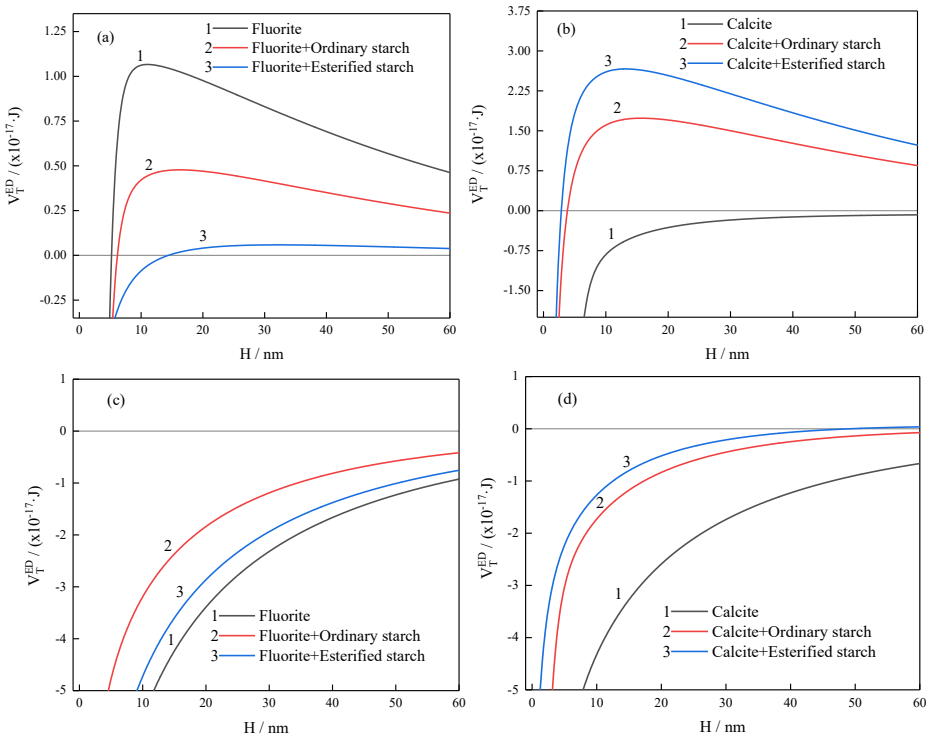

Fig. 11. Changes in total potential energy between particles before and after starch action. (a) Fluorite - Fluorite; (b) Calcite - Calcite; (c) Fluorite - sodium oleate; (d) Calcite - sodium oleate

Fig. 11 (b) illustrates that before starch was added, the total potential energy between calcite particles was negative, causing the particles to agglomerate. However, after starch was added, the total potential energy increased, and beyond 3.5 nm, calcite particles showed good dispersibility, with a stronger dispersion effect of esterified starch. The peak on the total potential energy curve between particles is referred to as the barrier (Xia et al., 2002). Starch molecules were adsorbed on the surface of calcite particles, and the total potential energy barrier of calcite increased. The distance between particles that were easy to condense decreased, and the hydration effect was obvious; as the distance decreased, the repulsive force of the hydration film intensified, leading to considerable dispersion between particles (Shen, 2017).

Figs. 11 (c) and (d) show that the total potential energy between minerals and sodium oleate was negative before starch was added. Adding starch increased the total potential energy between sodium oleate particles and mineral particles, while the increase in total potential energy between sodium oleate and fluorite was small, resulting in a decrease in particle cohesion; however, the change was inconsiderable. Conversely, the total potential energy between sodium oleate and calcite substantially increased, causing a rapid decrease in particle cohesion and greatly reducing the recovery rate of calcite.

4. Conclusions

Mineral flotation tests indicated that both fluorite and calcite exhibited good floatability in the sodium oleate system. With an esterified starch dosage of 40 mg/L, the difference in recovery rate of a single mineral was the greatest. The acidity and alkalinity of the environment had considerably affected the recovery rate of fluorite, while alkaline conditions had little impact on the recovery rate of calcite. The mixed ore experiment demonstrated that esterified starch could improve both the grade and recovery rate of fluorite.

The surface tension of the solution could be increased after adding starch inhibitors compared to before adding them. Esterified starch reduced the contact angle of calcite, enhanced its hydrophilicity, and reduced the recovery rate. The surface potential of minerals was positive before the addition of starch. However, the negative surface potential of calcite was small after adding esterified starch, which was not conducive to binding with sodium oleate anions. At this point, the surface potential of fluorite remained positive, facilitating the effective separation of minerals.

After the interaction between minerals and esterified starch, calcite particles demonstrated good dispersibility, while the cohesion between calcite particles and sodium oleate particles decreased, while the effect of fluorite was opposite. Chemically adsorbed to calcite, esterified starch hindered the adsorption of sodium oleate and calcite, so calcite was inhibited. The interaction between the surface of fluorite and esterified starch involved electrostatic adsorption, while sodium oleate was chemically adsorbed on the surface of fluorite. Chemical adsorption was stronger than electrostatic adsorption, so sodium oleate could capture fluorite.

Acknowledgments

The authors gratefully acknowledge the financial support provided by “Inner Mongolia Autonomous Region Science and Technology plan Project (2021GG0438)” and “North rare earth project, Key technology research and development of soft magnetic material for Bayan Obo Mine high abundance mixed rare earth”.

References

CHEN F.F., GU W.X., ZHENG Q.R., BAO M.W., 2011. *Experimental Discussion on the Measurement of Liquid Surface Tension by the Ring Pulling Method*. Guangdong Chemical Industry, 38(06), 208-209.

CHEN G.D., 2019. *The Origin of Pauling's Chemical Bond Theory*. Chemical Bulletin, 82(06), 566-575.

CORPAS M.J.R., PEREZ A., NAVARRO D.R., AMOR C.C., MARTIN L.M.A., CALERO M., 2020. *Testing of New Collectors for Concentration of Fluorite by Flotation in Pneumatic (Modified Hallimond Tube) and Mechanical Cells.* Minerals, 10(5), 482-490

DONG A.Q., XIE J., WANG W.M., YU L.P., LIU Q., YIN Y.P., 2010. *A novel method for amino starch preparation and its adsorption for Cu(II) and Cr(VI)*. Journal of Hazardous Materials, 181(1–3), 448-454.

FENG Q.M., ZHOU Q.B., ZHANG G.F., LU Y.P., YANG S.Y., 2011. *The inhibitory mechanism of sodium hexametaphosphate on calcite*. Chinese Journal of Nonferrous Metals, 21(02), 436-441.

GAO Y.S., GAO Z.Y., SUN W., 2016. *Research and Progress on Anisotropy of Surface Properties of Fluorite.* The Chinese Journal of Nonferrous Metals, 26(02), 415-422.

GAO Y.S., GAO Z.Y., SUN W., YIN Z.G., WANG J.J., HU Y.H., 2018. *Adsorption of a novel reagent scheme on scheelite and calcite causing an effective flotation separation.* Journal of Colloid and Interface Science, 512(15), 39-46.

GAO Z.Y., WANG C., SUN W., GAO Y.S., KOWALCZUK P.B., 2021. *Froth flotation of fluorite: A review*. Advances in colloid and interface science, 290, 102382.

HADLER K., CILLIERS J.J., 2019. *The Effect of Particles on Surface Tension and Flotation Froth Stability*. Mining, Metallurgy & Exploration, 36(1), 63-69.

HU Y.H., GAO Z.Y., SUN W., LIU X.W., 2012. *Anisotropic surface energies and adsorption behaviors of scheelite crystal.* Colloids and Surfaces A: Physicochemical and Engineering Aspects, 415, 439-448.

HU Y.H., QIU G.Z., WANG D.Z., 1994. *Extended DLVO Theory and Application in Fine Particle Flotation Systems*. Journal of Zhongnan Institute of Mining and Metallurgy, (03), 310-314.

HU Y.H., QIU G.Z., WANG D.Z., 1993. *Theory and Application of Interface Polar Interaction in Fine Particle Flotation Systems.* Journal of Zhongnan Institute of Mining and Metallurgy, (06), 749-754.

HU Y.H., XU J., QIU G.Z., WANG D.Z., 1994. *Electrostatic and van der Waals interactions between particles in fine-grained flotation systems.* NonFerrous Mining and Metallurgy, (02), 16-21.

JANINE G., DAVID W., DAVIDE D.S., GUIDO P., RIGNANESE G.M., GEOFFROY H., 2020. *The Limited Predictive Power of the Pauling Rules*. Angewandte Chemie International Edition, 59(19), 7569-7575.

LEEUW N.H., PARKER S.C., RAO K.H., 1998. *Modeling the competitive adsorption of water and methanoic acid on calcite and fluorite surfaces*. Langmuir, 14(20), 5900-5906.

LI Y., LIU Q., XU S., 1996. *Adsorption characteristics and mechanism of starch polysaccharides on the surface of calcite and fluorite*. NonFerrous Metal, (01), 26-30+15.

LIN Q., WANG D.Z., 1994. *Synthesis of dialkyl thiophosphinic acid and its flotation performance for pyrite and arsenopyrite.* NonFerrous Metals, (04), 28-31

LIU W.G., DUAN H., LIU W.B., PENG X.Y., 2021. *Research status of spatial matching characteristics between flotation reagents and mineral surface adsorption.* Metal Mine, (12), 2-10.

LU Q.Q., HAN H.S., CHEN Z.F., LI W.H., XU D.G., MU Y.Y., LIU R.H., 2023. *The Mechanism and Application of Typical Organic Inhibitors in Flotation Separation of Fluorite and Calcite*. Metal Mine, (01), 216-222.

MANN S., 1988. Molecular recognition in biomineralization. Nature, 332(6160):119-124.

NING Y.Q., WANG J.W., HU H.Y., HUANG Z.Q., ZHANG Y.J., QIN Y.B., 2021. *Preparation and characterization of citric acid esterified resistant starch*. Food Technology, 46(05), 213-218.

REN L.Y., 2012. *The Interaction between Fine Cassiterite Particles and Bubbles and Its Influence on Flotation*. Central South University.

SHANG P.Q., JIAO S., QU Y.Y., LIU B.Q., GAO Y.Z., 2020. *Analysis of the supply and demand situation of world fluorite resources and suggestions for countermeasures.* Land and Resources Information, (10), 104-109.

SHEN Z., 2017. *Colloid and Surface Chemistry, 4th edn*. Chemical Industry Press, Beijing.

SUN R.F., LIU D., LIU Y.B., WANG D.Q., WEN S.M., 2021. *Pb-water glass as a depressant in the flotation separation of fluorite from calcite.* Colloids and Surfaces A: Physicochemical and Engineering Aspects, 629, 127447.

TIMOTHY N.H., ROBERT J.P., GEORGE V.F., GRAEME J.J., 2008. *The role of particles in stabilising foams and emulsions.* Advances in Colloid and Interface Science, 137(2), 57-81.

VILINSKA A., RAO K.H., 2011. *Surface thermodynamics and extended DLVO theory of Leptospirillum ferrooxidans cells' adhesion on sulfide minerals*. Mining, Metallurgy & Exploration, 28, 151–158.

WANG D.Q., 2023. *Application and inhibition mechanism of oxidized starch in flotation separation of fluorite and calcite.* Kunming University of Science and Technology.

WANG J.Z., YIN W.Z., LI Z., 2016. *Study on the Difference and Mechanism of Flotation Behavior between Scheelite and Calcite.* Mineral Protection and Utilization, (04), 37-40+46.

WANG J.J., ZHOU Z.H., GAO Y.S., SUN W., HU Y.H., GAO Z.Y., 2018. *Reverse flotation separation of fluorite from calcite: a novel reagent scheme.* Minerals, 8(8), 313.

WANG M.L., WANG H., ZHANG G.R., ZHANG A.R., HAN Y.X., 2021. *Evaluation of measurement uncertainty for indication error of surface tension meter.* Metrology Science and Technology, 65(10), 27-30.

WANG R.L., HAN H.S., SUN W.J., SUN W., ZHANG H.L., CHENG Y.B., 2023. *Selective inhibition behavior and mechanism of Al-starch complexes on fine-grained calcite in scheelite flotation*. Mineral protection and utilization, 43(05), 1-10

XIA Q.B., LI Z., QIU X.Y., DAI Z.L., 2002. *Study on the Dispersion Mechanism of Sodium Hexametaphosphate on Serpentine.* Mining and Metallurgical Engineering, (02), 51-54

XIE J.X., CHANG J.B., WANG X.M., 2001. *The Application of Infrared Spectroscopy in Organic Chemistry and Pharmaceutical Chemistry*. Science Press, Beijing.

YOUNG C.A., MILLR J.D., 2001. *Conformation of chemisorbed oleate at a calcite surface*. Mining, Metallurgy & Exploration, 18, 38–44.

YU M.J., 2008. *Study on Citric Acid Modified Pea Starch*. Tianjin University.

ZHANG J.X., WANG C.L., NIU F.S., GUO J.B., WANG W.Q., 2023. *Preparation and performance of ferric chloride starch composite flocculant.* Mineral resources, 1-10

ZHAO P., ZHEN H.Y., ZHANG X., WANG F., WANG Y.L., 2020. *Current Situation and Development Suggestions of China's Fluorite Industry Resources.* Chemical and Mineral Geology, 42(02), 178-183.

ZHONG H., DEQUAN E., DONG L., WEN L.Y., 2017. *Theoretical study on the poly(m-phenylene) derivatives with lower HOMO–LUMO gaps*. Synthetic Metals, 229, 16-21.

ZHU W.X., PAN J.H., YU X.Y., HE G.C., LIU C., YANG S.Y., ZENG Y.H., ZENG A., LIU T.T., 2021. *The flotation separation of fluorite from calcite using hydroxypropyl starch as a depressant*. Colloids and Surfaces A: Physicochemical and Engineering Aspects, 616, 126-168.